



## TECHNICAL NOTE

D-1341

### **EARTH SCAN ANALOG SIGNAL RELATIONSHIPS IN THE TIROS RADIATION EXPERIMENT AND THEIR APPLICATION TO THE PROBLEM OF HORIZON SENSING**

Barney J. Conrath  
Goddard Space Flight Center  
Greenbelt, Maryland

NATIONAL AERONAUTICS AND SPACE ADMINISTRATION  
WASHINGTON

June 1962

1. The first part of the document is a list of the names of the members of the committee.

2. The second part of the document is a list of the names of the members of the committee.

3. The third part of the document is a list of the names of the members of the committee.

4. The fourth part of the document is a list of the names of the members of the committee.

5. The fifth part of the document is a list of the names of the members of the committee.

6. The sixth part of the document is a list of the names of the members of the committee.

# **EARTH SCAN ANALOG SIGNAL RELATIONSHIPS IN THE TIROS RADIATION EXPERIMENT AND THEIR APPLICATION TO THE PROBLEM OF HORIZON SENSING**

by

Barney J. Conrath

*Goddard Space Flight Center*

## **SUMMARY**

The five-channel medium-resolution scanning radiometers employed in the TIROS meteorological satellites provide data applicable to the problems encountered in selecting the optimum spectral region for horizon sensor systems. Simultaneous measurements are made in five spectral regions which include—in addition to two reflected solar radiation channels—a water vapor absorption band (6.0 to 6.5  $\mu$ ), the atmospheric "window" (8 to 12  $\mu$ ), and thermal radiation (7 to 30  $\mu$ ). Six cases were chosen to cover the wide range of synoptic situations likely to be encountered. Data from the three thermal channels (in analog form) and the corresponding television pictures are presented in a manner allowing easy correlation of the thermal data with surface and cloud features. The data indicate that the spectral regions including the atmospheric "window" would, in general, be poorly suited for use in horizon sensor work, and that investigation of spectral regions not directly covered in the TIROS experiment, such as the 15  $\mu$  carbon dioxide band, would prove more profitable.



## CONTENTS

Summary . . . . .	i
INTRODUCTION . . . . .	1
INSTRUMENTATION AND CALIBRATION . . . . .	1
SELECTED EXAMPLES . . . . .	3
SUMMARY AND CONCLUSIONS . . . . .	14
References . . . . .	16



# **EARTH SCAN ANALOG SIGNAL RELATIONSHIPS IN THE TIROS RADIATION EXPERIMENT AND THEIR APPLICATION TO THE PROBLEM OF HORIZON SENSING**

by

Barney J. Conrath  
*Goddard Space Flight Center*

## **INTRODUCTION**

Three TIROS meteorological satellites have been placed into near-circular orbits by NASA, and several more are planned for the near future. TIROS I, launched on April 1, 1960, carried cloud cover television cameras. TIROS II and TIROS III were launched on November 23, 1960, and July 12, 1961, respectively. In addition to television cameras, the latter two satellites carried instrumentation for measuring radiation emitted and reflected by the earth and its atmosphere. The system aspect of the radiation experiment has been described by Bandeen, et al. (Reference 1).

One of the several types of satellite borne radiometers employed (References 2 and 3), is a five-channel medium-resolution scanning radiometer. This instrument's primary purpose is to obtain measurements applicable to problems in meteorology and atmospheric physics, such as albedo determination, heat balance, and cloud cover determinations at night or when other means of observation are not available. Some preliminary results obtained from these measurements have been published recently (References 4 and 5). In addition to the primary objectives of the experiment, there is considerable interest in applying the simultaneous measurements made in several spectral regions to problems encountered in the design of horizon sensor systems.

Two basic problems in selecting the best spectral region for a horizon sensor are the effects of cloud systems on the sensor's behavior and its dependence on the viewing angle (limb-darkening), especially at large angles. Several examples which are applicable to these problems have been chosen from the TIROS data and are presented in this paper to illustrate the typical behavior of the various channels under different synoptic situations.

## **INSTRUMENTATION AND CALIBRATION**

The scanning radiometer consists of a cluster of five sensors with coincident fields of view about five degrees wide at the half-power points of the response. The spectral regions covered by these five channels are:

- (1) 6.0 to 6.5 $\mu$ , the water vapor absorption band;
- (2) 8.0 to 12 $\mu$ , the atmospheric "window";
- (3) 0.25 to 6.0 $\mu$ , the total reflected solar radiation;
- (4) 7.0 to 30 $\mu$ , thermal radiation; and
- (5) 0.55 to 0.75 $\mu$ , the visible reference.

These figures are purely nominal. The effective spectral response curves of each channel are given in References 1 and 6.

The optical axis of the instrument points in two directions 180 degrees apart. By means of rotating choppers, the sensors are exposed in rapid succession to radiation from first one direction and then the other. The resulting output signal is proportional to the difference in flux received from the two directions. The optical axis is inclined 45 degrees to the satellite's spin axis; thus the radiometer scans the earth as the satellite rotates about its spin axis, and the orbital motion of the satellite provides the scan advance. Whenever one direction of the optical axis points toward the earth, the other direction is pointed toward outer space. Therefore, outer space can be used as a zero reference. The instrumentation is described completely in References 1 and 7.

The three thermal channels (1, 2 and 4) are calibrated by exposing the instrument to a blackbody source at various known temperatures. From these temperatures, the portion of the radiant emittance which falls within the spectral response of a given channel,  $\bar{W}$ , is computed by integrating the Planck function over the spectral response curve (Figure 1). Thus, the outputs of the thermal channels can be expressed in terms of either  $\bar{W}$  or the equivalent blackbody temperature. The visible channels are calibrated in a similar fashion by exposing the instrument to a target of known spectral radiant emittance. The calibration process is described in detail in Reference 6.

## SELECTED EXAMPLES

The following cases have been selected in an effort to provide examples which will be of interest in horizon sensor considerations. Several of the examples are from previously published case studies (Reference 5). In all cases, the data shown are from TIROS III.

Where possible, examples have been chosen for which television coverage exists. The pictures have been gridded in terms of geographic longitude and latitude, and the radiometer scan paths on the earth's surface have been drawn. Analog oscillograms of the radiometer output for these scan paths are included. Arbitrary angles of satellite rotation are indicated along the scans in the television pictures and along the abscissas in the oscillograms. Thus, points along a scan may be correlated with corresponding points on the oscillogram. The ordinates of the oscillograms are given in terms of effective radiant emittance  $\bar{W}$ .



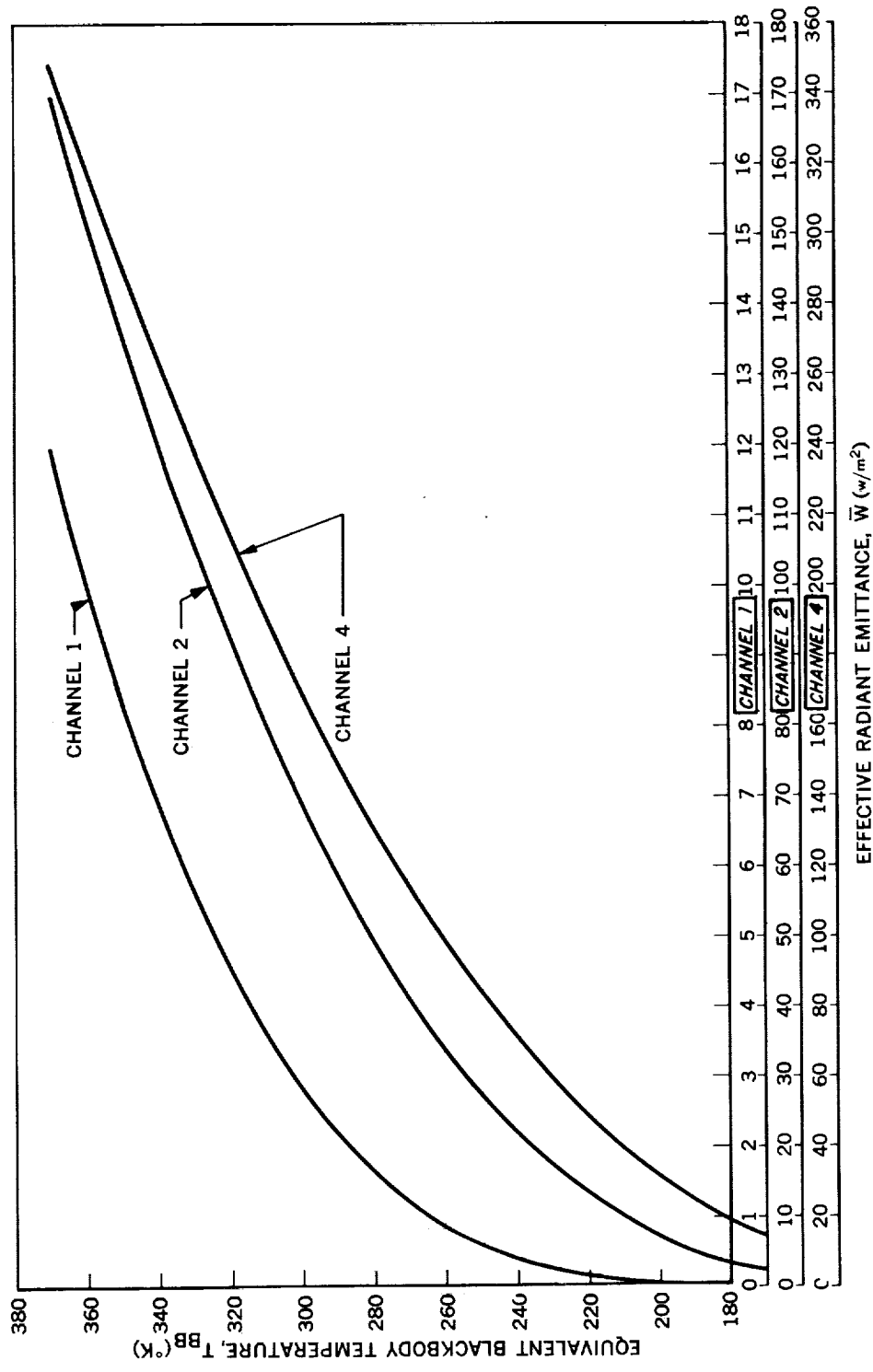


Figure 1 - The effective radiant emittance versus the equivalent blackbody temperature for the three thermal channels used on TIROS III. The curves are obtained by integrating the product of the Planck function and the spectral response curves over all wavelengths.

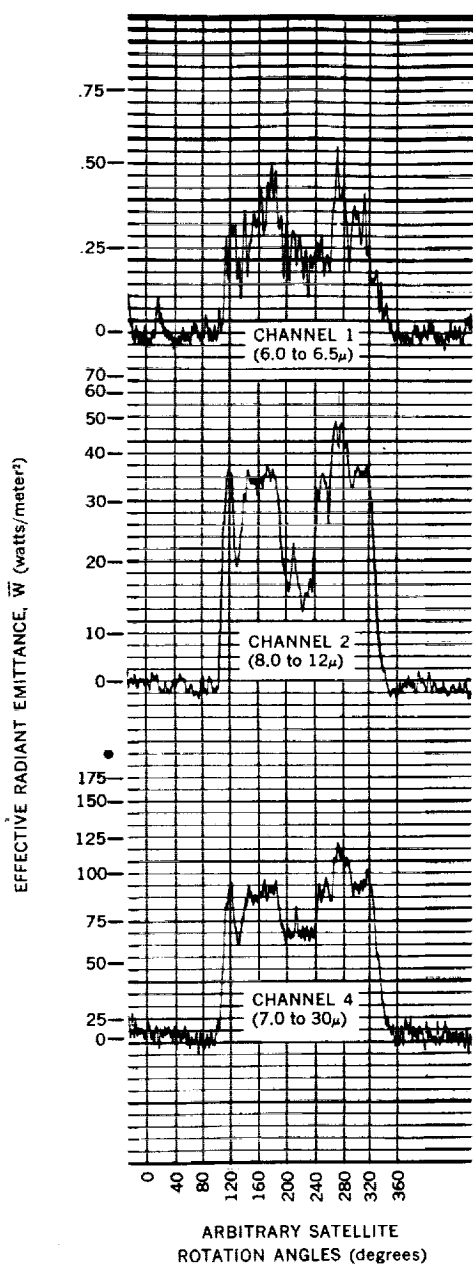


Figure 2 - Analog oscillogram of the outputs of the three thermal channels showing the data discussed in Example 1.

### Example 1

The first example is taken from one of three case studies previously described in Reference 5. Figure 2 shows the oscillogram of the three thermal channels corresponding to the scan path indicated on the photograph in Figure 3. A large cloud mass is prominent near the center of the picture, with a clear area over the Great Lakes and the Michigan peninsula in the upper left corner.

The situation illustrates the behavior of the sensors when scanning an extensive cloudy region of fairly high albedo. This was the largest area of solid cloud cover that could be found in a search of the pictures from the first 200 orbits of TIROS III. The maximum albedo measured in this area was about 55 percent in the 0.55 to 0.75 $\mu$  region.

The most obvious feature of this example is the large decrease in radiant emittance seen in all three thermal channels as the cloud mass is scanned. The radiation gradients viewed through the TIROS 5-degree fields of view are quite steep in the 7 to 30 $\mu$  channel and especially in the 8 to 12 $\mu$  channel where they are equal in magnitude to the horizon gradients. The gradients in the 6.0 to 6.5 $\mu$  channel are somewhat less steep. It is not possible to show the entire area covered by a radiometer scan path in a single television picture, hence, conditions near the points where the scan path intersects the horizon cannot be seen here. However, it is probable that the horizon was clear at the points of intersection since no strong signals were observed in the visible channels and the weather map shows no overcast in these regions.

G-241

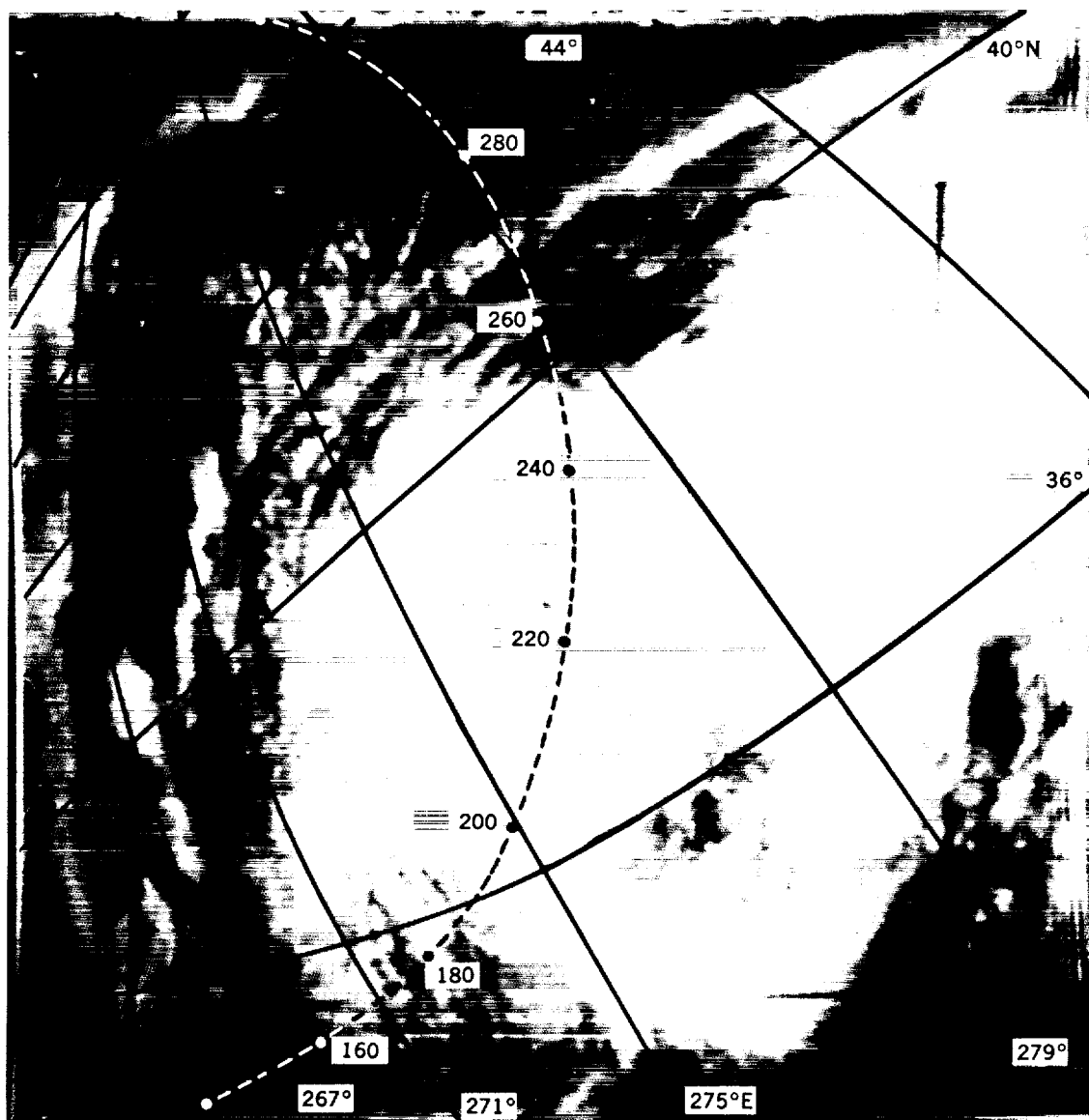


Figure 3 - Photograph taken by TIROS III at about 1735 GMT on July 12, 1961. Michigan and the Great Lakes are visible in the upper left corner. The radiometer scan path (dashed), with arbitrary satellite rotation angles, is shown crossing the large central cloud mass.

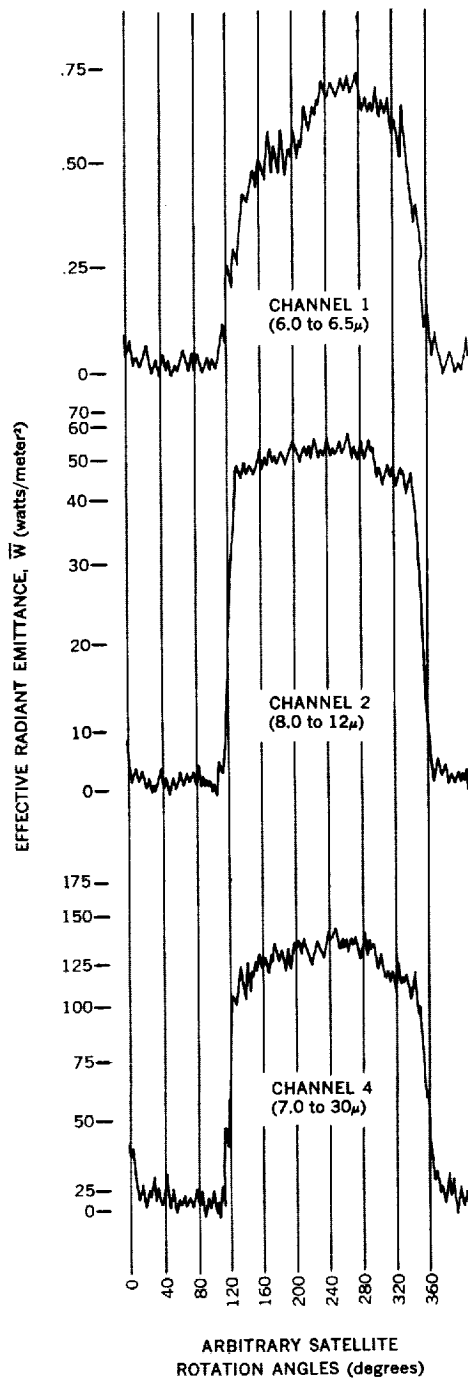


Figure 4 - Analog oscillogram showing the data from the three thermal channels discussed in Example 2.

## Example 2

The second example, also taken from Reference 5, is concerned with data taken over the Libyan desert. The oscillogram is shown in Figure 4 and the television picture in Figure 5. The brighter areas are sand-covered for the most part, having albedos of 27 or 28 percent as measured by the  $0.55$  to  $0.75\mu$  channel. This region is apparently totally free from cloudiness.

The oscillogram (Figure 4) of the scan path, especially between 200 and 280 degrees of satellite rotation, illustrates the behavior of the thermal channels over a region of what must be fairly uniform radiant emittance. In this region, the effective blackbody temperatures deduced from the  $8$  to  $12\mu$  channel are around  $310^\circ\text{K}$ , which is near the channel's saturation point. The high response observed in the  $6.0$  to  $6.5\mu$  channel indicates the absence of any large amount of water vapor in this area.

At angles of satellite rotation less than 200 degrees, the radiometer was viewing the uplands region near the border of Libya and Chad. The most outstanding feature of this region is the lower radiant emittance values viewed by channel 1, which indicate a higher atmospheric water vapor content. Near 295 degrees of satellite rotation, the transition from land to water shows up sharply in channels 2 and 4.

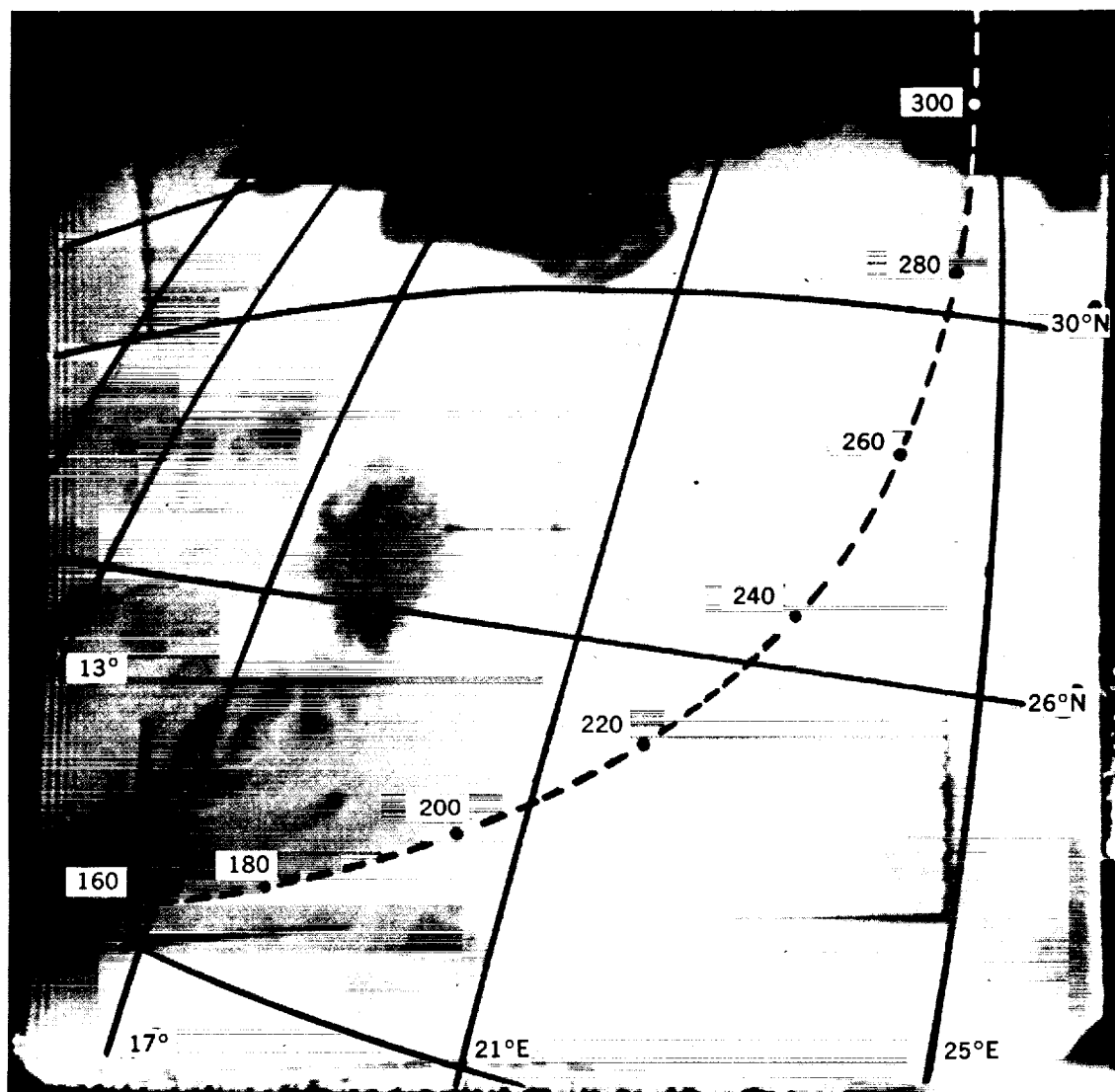


Figure 5 - Photograph taken over Libya by TIROS III at about 1053 GMT on July 15, 1961. The North African coast line and the Mediterranean Sea are visible near the top of the picture.

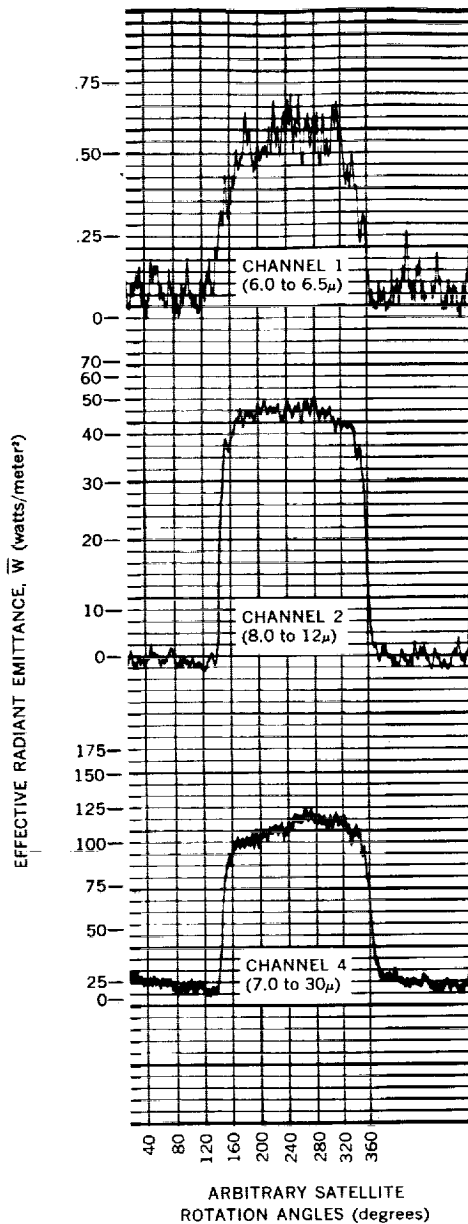


Figure 6 - Analog oscillogram showing the data from the three thermal channels discussed in Example 3.

### Example 3

The following example, also from Reference 5, was chosen to illustrate the behavior of the sensors over a relatively clear tropical ocean. The data were taken by TIROS III off the northern coast of South America. The oscillogram is shown in Figure 6, and the television picture in Figure 7. The coast line of the Guianas, partially obscured by clouds, can be seen in the upper left-hand corner of Figure 7.

The albedo measured by channels 3 and 5 is quite low over this area, as would be expected. However, the effective blackbody temperature obtained from the 8 to 12μ channel is about 20°K lower than the expected surface temperature of the water in this region. This is probably caused, in part, by residual water vapor absorption in the atmospheric "window", since soundings at Trinidad indicated over 5 centimeters of precipitable water vapor. Other contributing factors may be the presence of high cirrus clouds (which do not show in the television picture) or the presence of other absorbers, such as aerosols.

If it is assumed that the area covered by this scan path is fairly uniform in radiant emittance as the picture would seem to indicate, this case provides a good example of the variation of the sensor output with viewing angle. At the center of the scan, the zenith angle (at the spot viewed) is near zero. This angle increases in either direction from the center of the scan, approaching 90 degrees at each horizon. The apparent limb-darkening is least for the 8 to 12μ channel and greatest for the 6.0 to 6.5μ channel.

G-241

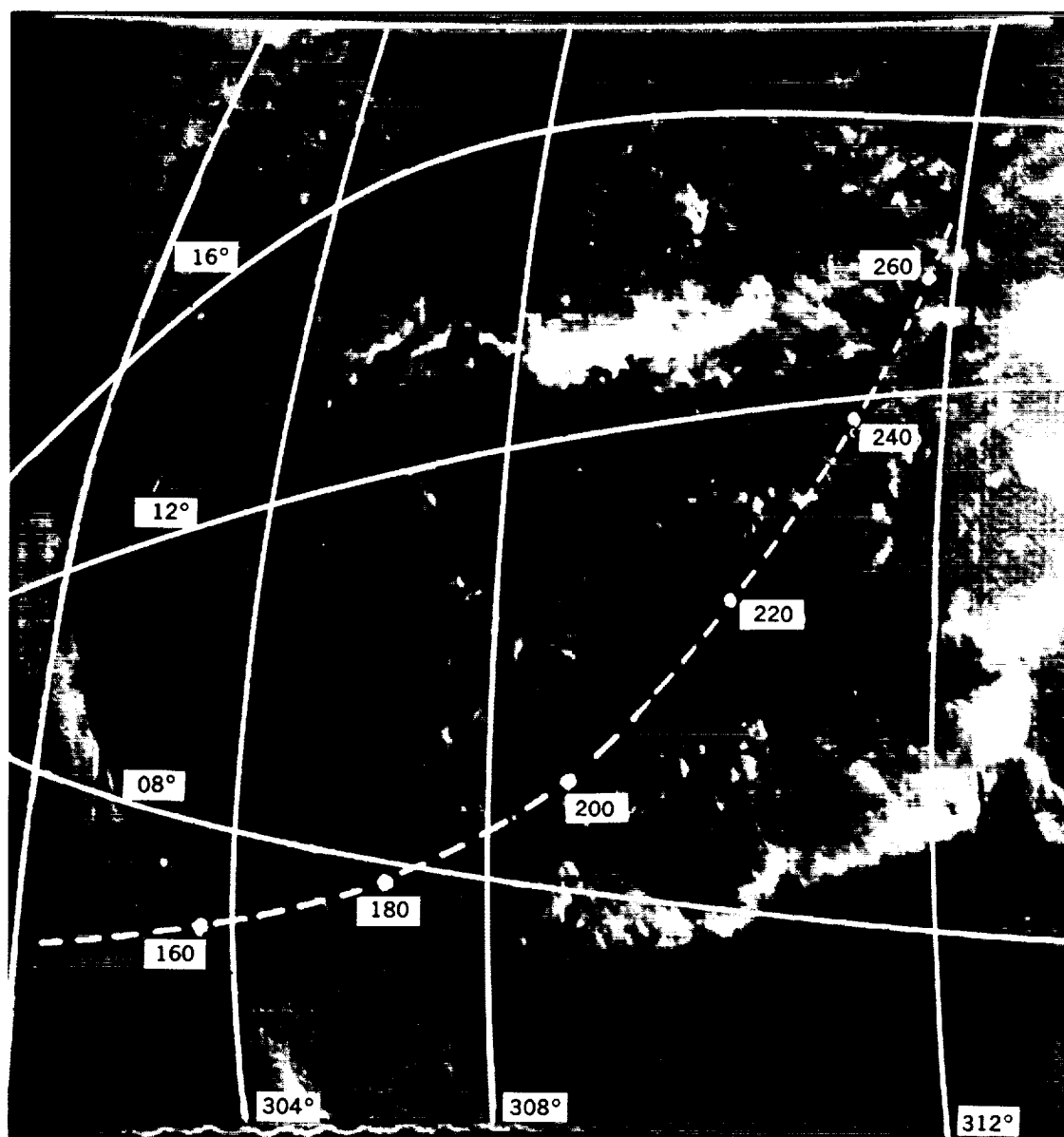


Figure 7 - Photograph taken off the northern coast of South America by TIROS III at about 1444 GMT on July 20, 1961. The partially cloud covered coast line of the Guianas is seen in the lower left corner.

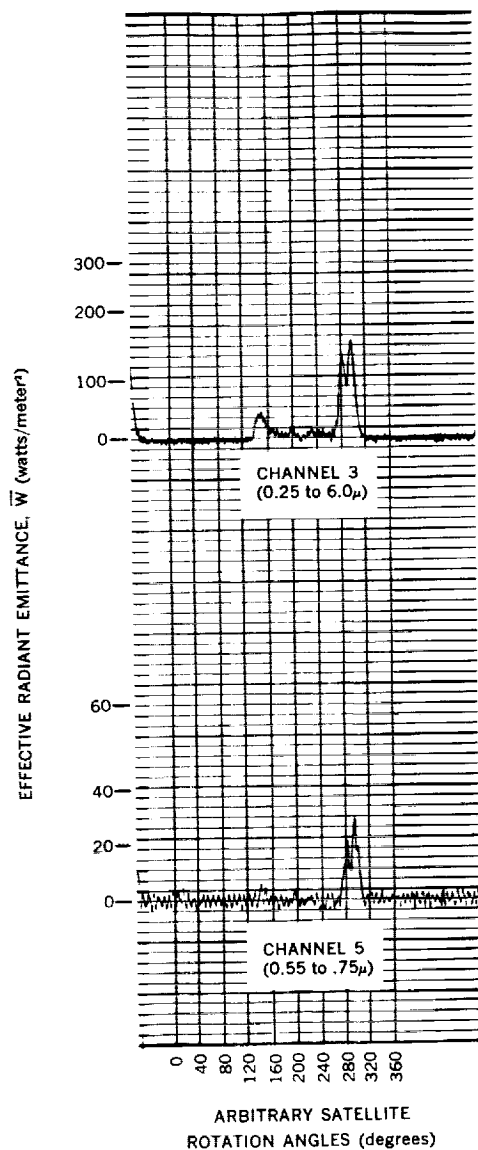


Figure 8 - Analog oscillogram showing the data from the two visible channels discussed in Example 4.

#### Example 4

The next case illustrates the behavior of the sensors as a cloudy horizon is scanned. The oscillograms of the visible channels (3 and 5) have been included in place of television pictures since it is difficult to determine the conditions near the horizon from the pictures with any certainty.

This scan path begins at a point off the eastern coast of Florida and terminates in Canada about 50°N and 70°W north of Maine. The visible channels (Figure 8) show relatively strong signals in the latter region (between 280 and 320 degrees of satellite rotation), which would indicate the presence of clouds on this horizon. In addition, data from the northern hemisphere surface chart (Figure 9) indicate a low pressure area and stationary front with associated cloudiness in this region. In the thermal channel oscillograms (Figure 10), the 8 to 12 $\mu$  channel shows the largest relative decrease in amplitude. The 7 to 30 $\mu$  channel shows less decrease, and the effect is almost lost in the 6.3 $\mu$  channel owing to the large dependence of this channel on the viewing angle. The remainder of the scan between 140 and 280 degrees of satellite rotation is over clear ocean with occasional broken cloudiness.



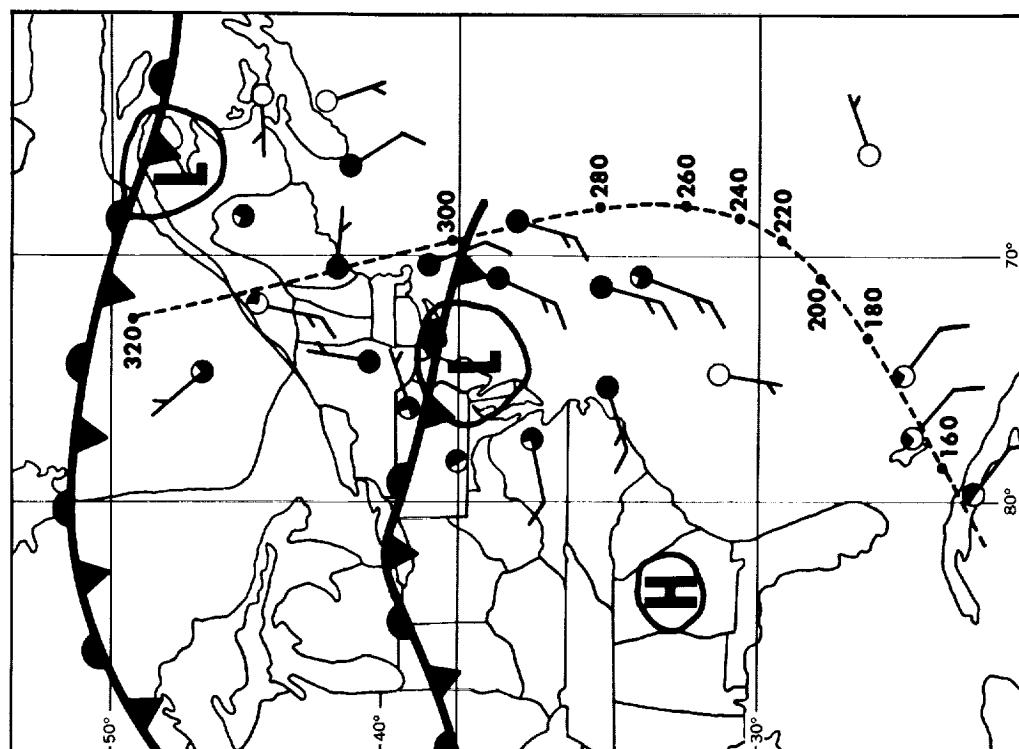


Figure 9 - Map showing data taken from the northern hemisphere surface chart for 1800 GMT on July 17, 1961. The broken line shows the satellite scan path discussed in Example 4.

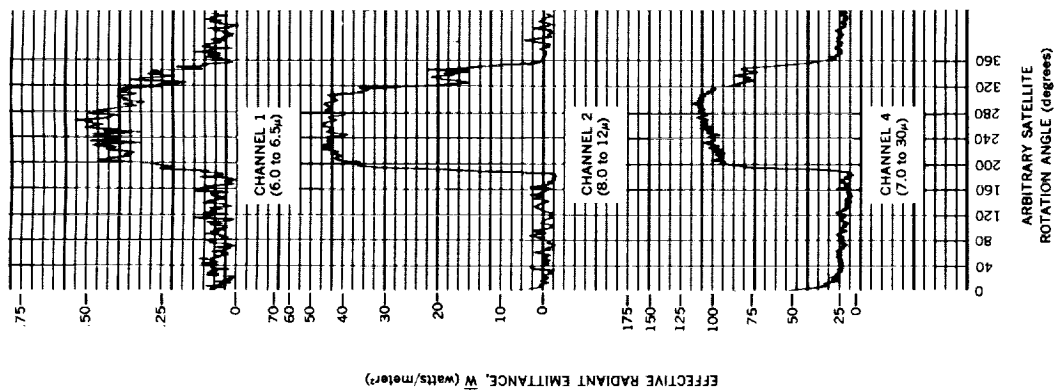


Figure 10 - Analog oscillogram showing the data from the three thermal channels discussed in Example 4.

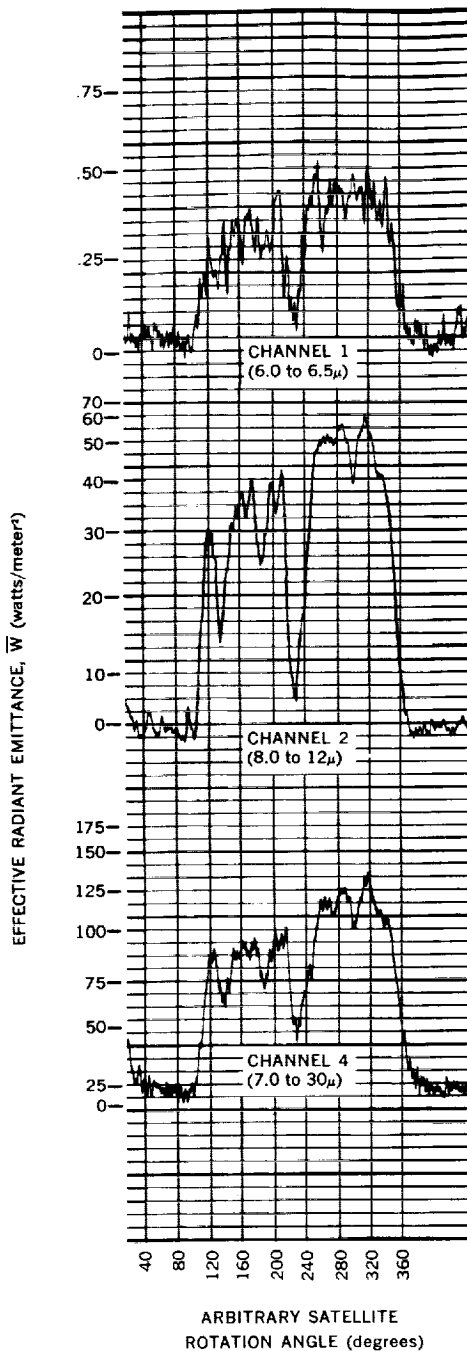


Figure 11 - Analog oscillogram showing the thermal data discussed in Example 5.

### Example 5

The next example concerns data acquired on July 17, 1961, at about 1308 GMT over north-west Africa. The analog oscillograms for the thermal channels are shown in Figure 11, and the picture of the region, containing part of the African coast line and the Atlantic Ocean, in Figure 12. That portion of the cloud system intersected by the scan path displayed the highest albedo found in a search of all TIROS III radiation data for which corresponding television pictures existed. The maximum measured albedo was 62 percent in the 0.55 to 0.75μ region.

The oscillograms show a narrow but very deep minimum at a rotation angle of about 220 degrees, which corresponds to the region of maximum observed albedo. The thermal channels show a reversal of their normal pattern in that Channel 1 shows the highest equivalent blackbody temperature, followed by Channel 4, with Channel 2 the lowest. This indicates a very high cloud, probably near the tropopause. In this example, the profile of the Channel 1 analog more closely follows those of the other two channels than in the previous cases. Channel 2 again shows the sharpest gradients, while those of Channel 4 are less acute.

For rotation angles of less than 200 degrees, the pattern is typical for a region of broken cloudiness. At angles greater than 260 degrees, the sensors are probably viewing a vegetated area that is relatively cloud-free.

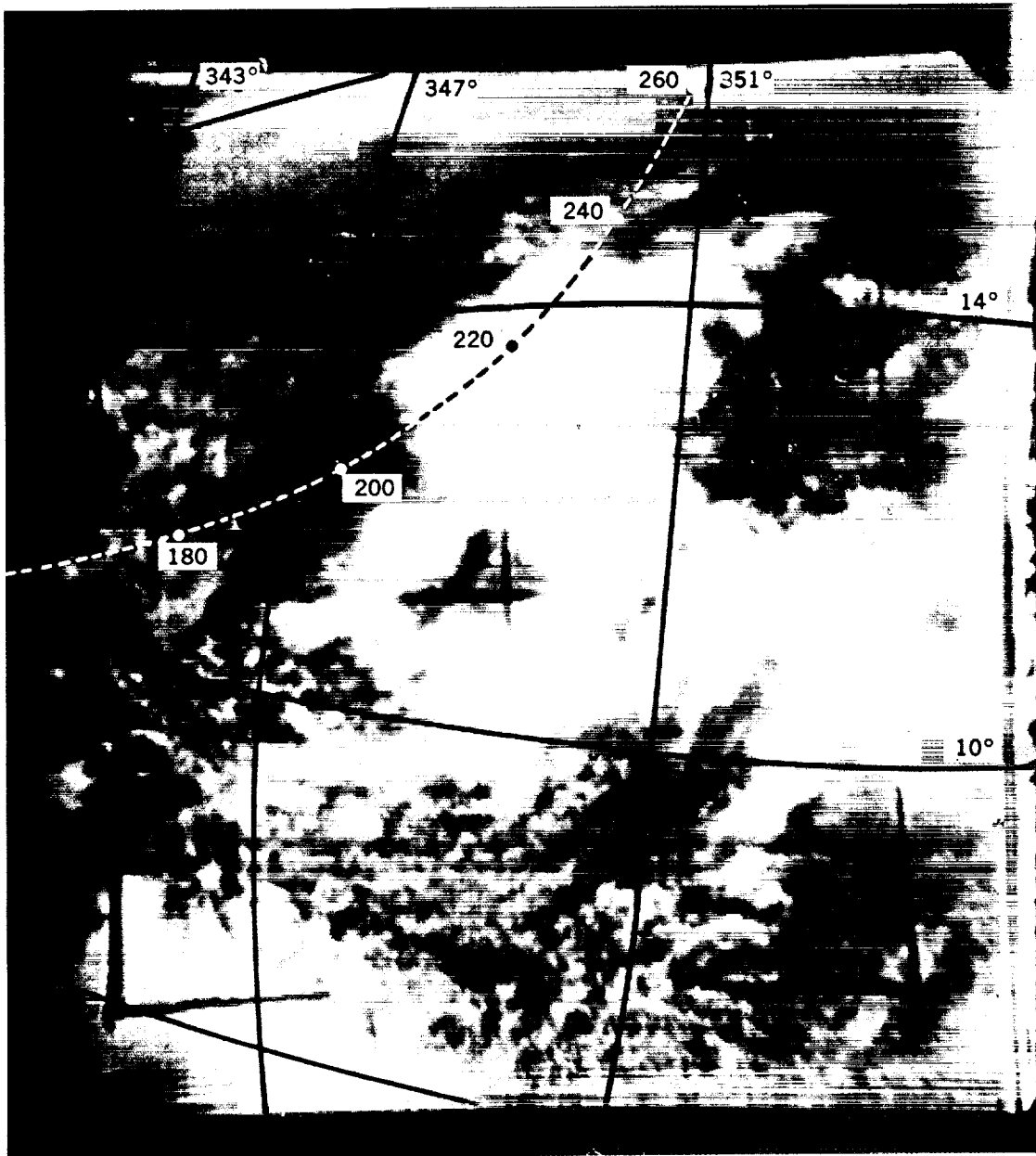


Figure 12 - Photograph taken over northwest Africa by TIROS III at about 1309 GMT on July 17, 1961. The African coast line and the Atlantic Ocean can be seen in the upper left corner.

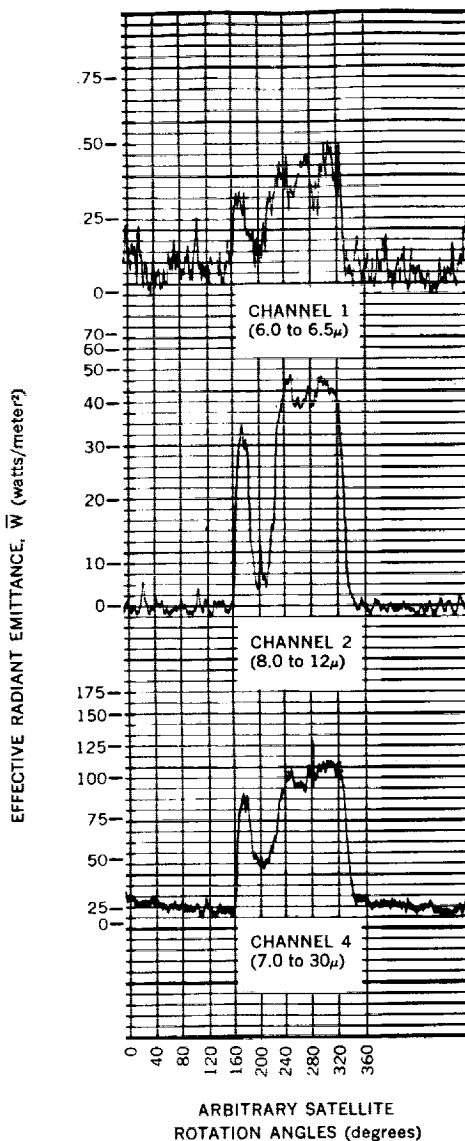


Figure 13 - Analog oscillogram of the thermal data discussed in Example 6.

(Figure 6). This effect is expected to be greatest in the tropical atmosphere and least in the arctic atmosphere (Reference 8). Another disadvantage of this spectral region is the small amount of total radiant power available, which leads to instrumentation difficulties in obtaining a good signal-to-noise ratio.

The 8 to 12 $\mu$  channel shows an excellent response to the horizon with steep gradients and little limb-darkening. In addition, there is no signal-to-noise problem because of the large amount of total radiant power available. However, the pronounced reaction to the presence

## Example 6

The data presented in this final example were taken by TIROS III over the Caribbean on July 22, 1961, at about 1512 GMT. Figure 13 shows the analog oscillograms of the three thermal channel outputs as the radiometer scanned the path seen in Figure 14. The cloud system associated with Hurricane Anna occupies the central portion of the picture; Florida and the Gulf of Mexico lie to the upper left.

## SUMMARY AND CONCLUSIONS

It would be possible to choose examples illustrating sensor behavior under many conditions, but the above cases cover a sufficiently wide range to provide some feeling for the characteristics of the various spectral regions. Examples 1, 2, 3, and 4 may be considered typical of the situations described. The extent of the cloud system in Example 1 is probably somewhat greater than might normally be expected, but the behavior of the sensors can be considered typical. Although the synoptic situations illustrated in Examples 5 and 6 are relatively rare, they show the extreme effects that isolated storm centers can produce in the infrared output.

The 6.0 to 6.5 $\mu$  region has a serious disadvantage in that it usually displays severe limb-darkening. This is noticeable in all of the examples, but is best illustrated in Example 3

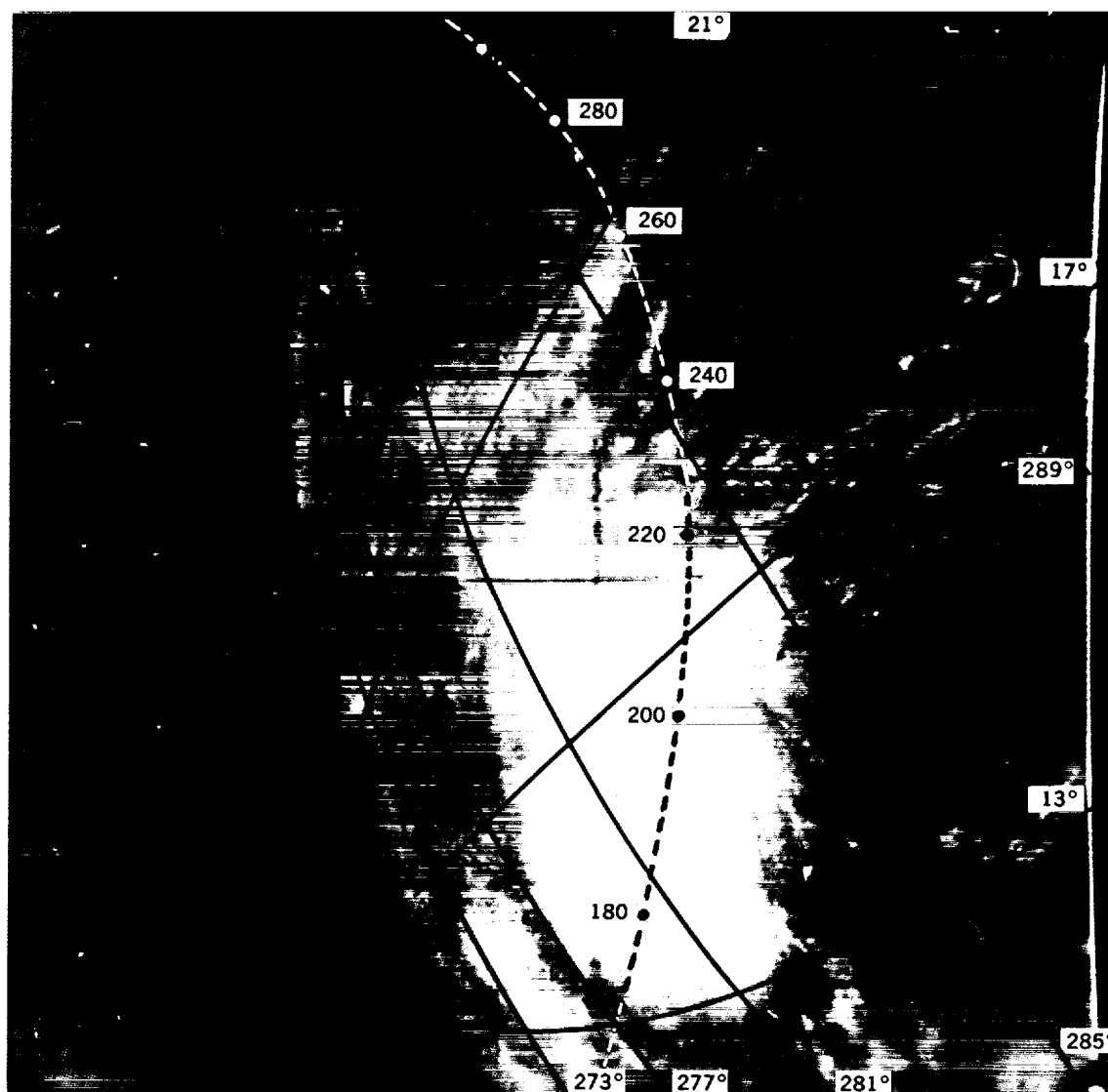


Figure 14 - Photograph of Hurricane Anna taken by TIROS III at about 1512 GMT on July 22, 1961. Cuba and Florida can be seen to the north of the storm center.

of clouds almost certainly makes this spectral region unsuitable for use in horizon sensor work, as Examples 1, 4, 5 and 6 well illustrate. The gradients displayed as the sensor scans the cloud systems are as steep as those resulting from the horizon itself, and in the case of very high clouds, as in Examples 5 and 6, the signal can plunge almost to the noise level.

The 7 to 30  $\mu$  channel is affected by limb-darkening only slightly more than the 8 to 12  $\mu$  channel, and ample total radiant power is available. Since the atmospheric "window" is also included in this spectral region, the signal is considerably affected by cloud systems. However, this effect is somewhat more moderate here than in the 8 to 12  $\mu$  region as Examples 1, 5 and 6 demonstrate. In general, although the gradients are not as steep and the drops in radiation level when scanning clouds are not as severe, these effects will continue to cause serious problems.

The TIROS data indicate that the final choice of an optimum spectral region should be one which does not include the atmospheric "window". In fact, it would seem more profitable to investigate spectral regions not directly covered in the TIROS experiments, such as the  $15\mu$  carbon dioxide band.

#### REFERENCES

1. Bandeen, W. R., Hanel, R. A., Licht, J., Stampfl, R. A., and Stroud, W. G., "Infrared and Reflected Solar Radiation Measurements from the Tiros II Meteorological Satellite," J. Geophys. Res. 66 (10):3169-3185, October 1961; also NASA Technical Note D-1069, November 1961
2. Hanel, R. W., "Low Resolution Unchopped Radiometer for Satellites," ARS J. 31 (2): 246-250, February 1961; also NASA Technical Note D-485, February 1961
3. Astheimer, R. W., DeWaard, R., and Jackson, E. A., "Infrared Radiometric Instruments on TIROS II," J. Optical Soc. Amer. 51 (12):1386-1393, December 1961
4. "TIROS II Radiation Data Catalog," Vol. I, NASA, Goddard Space Flight Center, August 15, 1961
5. Nordberg, W., Bandeen, W. R., Conrath, B. J., Kunde, V., and Persano, I., "Preliminary Results of Radiation Measurements from the TIROS III Meteorological Satellite," J. Atmospheric Sciences 19 (1):20-30, January 1962; also NASA Technical Note D-1338, in publication, 1962
6. "TIROS II Radiation Data Users' Manual," NASA, Goddard Space Flight Center, August 15, 1961
7. Davis, J., Hanel, R. A., Stampfl, R. A., Strange, M., and Townsend, M., "Telemetering IR Data from the TIROS II Meteorological Satellite," Paper presented at the 6th National Symposium on Space Electronics and Telemetry, Albuquerque, N. M., September 1961; also NASA Technical Note D-1293, in publication, 1962
8. Hanel, R. A. and Wark, D. Q., "TIROS II Radiation Experiment and Its Physical Significance," J. Optical Soc. Amer. 51 (12):1394-1399, December 1961; also NASA Technical Note D-701, December 1961

<p>NASA TN D-1341 National Aeronautics and Space Administration. EARTH SCAN ANALOG SIGNAL RELATIONSHIPS IN THE TIROS RADIATION EXPERIMENT AND THEIR APPLICATION TO THE PROBLEM OF HORIZON SENSING. Barney J. Conrath. June 1962. 16p. OTS price, \$0.50. (NASA TECHNICAL NOTE D-1341)</p> <p>The five-channel medium-resolution scanning radiometers employed in the TIROS meteorological satellites provide data applicable to the problems encountered in selecting the optimum spectral region for horizon sensor systems. Simultaneous measurements are made in five spectral regions which include - in addition to two reflected solar radiation channels - a water vapor absorption band (6.0 to 6.5<math>\mu</math>), the atmospheric "window" (8 to 12<math>\mu</math>), and thermal radiation (7 to 30<math>\mu</math>). Six cases were chosen to cover the wide range of synoptic situations likely to be encountered. Data from the three thermal channels (in analog form) and the corresponding television (over)</p>	<p>I. Conrath, Barney J. II. NASA TN D-1341</p> <p>(Initial NASA distribution: 17, Communications and sensing equipment, flight; 19, Electronics; 22, Guidance and homing systems; 29, Navigation and navigation equipment; 46, Space mechanics; 49, Simulators and computers.)</p>	NASA
<p>NASA TN D-1341 National Aeronautics and Space Administration. EARTH SCAN ANALOG SIGNAL RELATIONSHIPS IN THE TIROS RADIATION EXPERIMENT AND THEIR APPLICATION TO THE PROBLEM OF HORIZON SENSING. Barney J. Conrath. June 1962. 16p. OTS price, \$0.50. (NASA TECHNICAL NOTE D-1341)</p> <p>The five-channel medium-resolution scanning radiometers employed in the TIROS meteorological satellites provide data applicable to the problems encountered in selecting the optimum spectral region for horizon sensor systems. Simultaneous measurements are made in five spectral regions which include - in addition to two reflected solar radiation channels - a water vapor absorption band (6.0 to 6.5<math>\mu</math>), the atmospheric "window" (8 to 12<math>\mu</math>), and thermal radiation (7 to 30<math>\mu</math>). Six cases were chosen to cover the wide range of synoptic situations likely to be encountered. Data from the three thermal channels (in analog form) and the corresponding television (over)</p>	<p>I. Conrath, Barney J. II. NASA TN D-1341</p> <p>(Initial NASA distribution: 17, Communications and sensing equipment, flight; 19, Electronics; 22, Guidance and homing systems; 29, Navigation and navigation equipment; 46, Space mechanics; 49, Simulators and computers.)</p>	NASA
<p>NASA TN D-1341 National Aeronautics and Space Administration. EARTH SCAN ANALOG SIGNAL RELATIONSHIPS IN THE TIROS RADIATION EXPERIMENT AND THEIR APPLICATION TO THE PROBLEM OF HORIZON SENSING. Barney J. Conrath. June 1962. 16p. OTS price, \$0.50. (NASA TECHNICAL NOTE D-1341)</p> <p>The five-channel medium-resolution scanning radiometers employed in the TIROS meteorological satellites provide data applicable to the problems encountered in selecting the optimum spectral region for horizon sensor systems. Simultaneous measurements are made in five spectral regions which include - in addition to two reflected solar radiation channels - a water vapor absorption band (6.0 to 6.5<math>\mu</math>), the atmospheric "window" (8 to 12<math>\mu</math>), and thermal radiation (7 to 30<math>\mu</math>). Six cases were chosen to cover the wide range of synoptic situations likely to be encountered. Data from the three thermal channels (in analog form) and the corresponding television (over)</p>	<p>I. Conrath, Barney J. II. NASA TN D-1341</p> <p>(Initial NASA distribution: 17, Communications and sensing equipment, flight; 19, Electronics; 22, Guidance and homing systems; 29, Navigation and navigation equipment; 46, Space mechanics; 49, Simulators and computers.)</p>	NASA
<p>NASA TN D-1341 National Aeronautics and Space Administration. EARTH SCAN ANALOG SIGNAL RELATIONSHIPS IN THE TIROS RADIATION EXPERIMENT AND THEIR APPLICATION TO THE PROBLEM OF HORIZON SENSING. Barney J. Conrath. June 1962. 16p. OTS price, \$0.50. (NASA TECHNICAL NOTE D-1341)</p> <p>The five-channel medium-resolution scanning radiometers employed in the TIROS meteorological satellites provide data applicable to the problems encountered in selecting the optimum spectral region for horizon sensor systems. Simultaneous measurements are made in five spectral regions which include - in addition to two reflected solar radiation channels - a water vapor absorption band (6.0 to 6.5<math>\mu</math>), the atmospheric "window" (8 to 12<math>\mu</math>), and thermal radiation (7 to 30<math>\mu</math>). Six cases were chosen to cover the wide range of synoptic situations likely to be encountered. Data from the three thermal channels (in analog form) and the corresponding television (over)</p>	<p>I. Conrath, Barney J. II. NASA TN D-1341</p> <p>(Initial NASA distribution: 17, Communications and sensing equipment, flight; 19, Electronics; 22, Guidance and homing systems; 29, Navigation and navigation equipment; 46, Space mechanics; 49, Simulators and computers.)</p>	NASA

NASA TN D-1341

pictures are presented in a manner allowing easy correlation of the thermal data with surface and cloud features. The data indicate that the spectral regions including the atmospheric "window" would, in general, be poorly suited for use in horizon sensor work, and that investigation of spectral regions not directly covered in the TIROS experiment, such as the  $15\mu$  carbon dioxide band, would prove more profitable.

NASA

NASA

NASA TN D-1341

pictures are presented in a manner allowing easy correlation of the thermal data with surface and cloud features. The data indicate that the spectral regions including the atmospheric "window" would, in general, be poorly suited for use in horizon sensor work, and that investigation of spectral regions not directly covered in the TIROS experiment, such as the  $15\mu$  carbon dioxide band, would prove more profitable.

NASA

NASA

NASA TN D-1341

pictures are presented in a manner allowing easy correlation of the thermal data with surface and cloud features. The data indicate that the spectral regions including the atmospheric "window" would, in general, be poorly suited for use in horizon sensor work, and that investigation of spectral regions not directly covered in the TIROS experiment, such as the  $15\mu$  carbon dioxide band, would prove more profitable.

NASA TN D-1341

pictures are presented in a manner allowing easy correlation of the thermal data with surface and cloud features. The data indicate that the spectral regions including the atmospheric "window" would, in general, be poorly suited for use in horizon sensor work, and that investigation of spectral regions not directly covered in the TIROS experiment, such as the  $15\mu$  carbon dioxide band, would prove more profitable.